

JOINT TIME-FREQUENCY REPRESENTATION OF NON-STATIONARY SIGNALS IN ELECTRICAL POWER ENGINEERING

Tadeusz Lobos*, Tomasz Sikorski*, Peter Schegner#

* Dept. of Electrical Engineering, Wrocław University of Technology, Wyb. Wyspińskiego 27, 50-370 Wrocław POLAND, tadeusz.lobos@pwr.wroc.pl, tomasz.sikorski@pwr.wroc.pl

#Inst. of Electrical Power System and High Voltage Technology, Dresden University of Technology, 01062 Dresden GERMANY, schegner@ieeh.et.tu-dresden.de

Abstract – This paper provides an idea of applying the nonparametric, bilinear time-frequency representations for analysis of non-stationary signals in electrical engineering. Winger-Ville (WVD), Choi-Williams (CWD), Zhao-Atlas-Marks (ZAMD) distributions and its smoothed versions were performed with comparison to short-time Fourier transform (STFT). To investigate the methods several experiments were performed using real measured dc arc furnaces signal and simulated faults signal in transmission line. Proposed methods allowed to track instantaneous frequency as well as magnitude. The local frequency moments are also introduced as one-dimensional characteristic for classification and diagnosis area.

Keywords: Power system harmonics, signal analysis, time-frequency analysis, fault diagnosis.

1 INTRODUCTION

Nonstationarity brings a new challenges for signal processing area. Natural direction to calculate only the spectrum of the signal can be insufficient, providing only general information with loss of time-varying nature of analysed phenomena. The violation of main assumption of spectral analysis, the stationarity, can be solved by introducing the joint time-frequency domain.

The standard method for study time-varying signals is the short-time Fourier transform (STFT) that is based on the assumption that for a short-time basis signal can be considered as stationary [10]. The spectrogram utilizes a short-time window whose length is chosen so that over the length of the window signal is stationary. Then, the Fourier transform of this windowed signal is calculated to obtain the energy distribution along the frequency direction at the time corresponding to the centre of the window. The crucial drawback of this method is that the length of the window is related to the frequency resolution. Increasing the window length leads to improving frequency resolution but it means that the non-stationarities occurring during this interval will be smeared in time and frequency. This inherent relationship between time and frequency resolution becomes more important when one is dealing with signals whose frequency content is changing rapidly. A time-frequency characterization that would overcome above drawback became a major goal for alternative development based on non-parametric, bilinear transformations.

The first suggestions for designing non-parametric, bilinear transformations were introduced by Wigner,

Ville and Moyal at the begging of nineteen-forties in the context of quantum mechanics area. Next two decades beard fruit of significant works by Page, Rihaczek, Levin, Mark, Choi and Williams, Born and Jordan, who provided unique ideas for time-frequency representations, especially reintroduced to signal analysis [4], [5]. At last in nineteen-eighties Leon Cohen employed concept of kernel function and operator theory to derive a general class of joint time-frequency representation [3]. It can be shown that many bilinear representations can be written in one general form that is traditionally named Cohen's class, Figure 1.

Following Cohen's idea we can reveal the main motivation for devising a joint time-frequency distribution (TFC). Having such function it can be found what fraction of energy is in a certain frequency and time range, it can be calculated the distribution of frequency at particular time, the global and local moments of the distribution such as the mean frequency and its local spread. The fundamental goal is to devise a joint function of time and frequency, which represents the energy or intensity per unit time and per unit frequency. Such joint distribution $TFC(t, \omega)$ means intensity at time t and frequency ω or $TFC(t, \omega)\Delta t\Delta \omega$ means fractional energy in time-frequency cell $\Delta t\Delta \omega$ at t, ω . For deterministic signals where no probabilistic consideration enter, the distribution can be treated as intensities or densities which shows how the energy is distributed in the time-frequency cells. In order to achieve above goal two main conditions must be fulfilled. Time marginal condition, concerning the instantaneous energy of signal $x(t)$, and frequency marginal conditions which lead to energy density spectrum. Only then total energy of analysed signal would be preserved [3], [5]:

$$\int_{-\infty}^{\infty} TFC(t, \omega) d\omega = |x(t)|^2 \quad (1)$$

$$\int_{-\infty}^{\infty} TFC(t, \omega) dt = |X(\omega)|^2 \quad (2)$$

Although the main directions of time-frequency representation has evaluated since nineteen-forties only present increase of computational power made them attractive and possible to apply. The main novel fields of application consist speech processing, seismic, economic and biomedical data analysis [1], [9], [10]. Recently some efforts was also made to introduce time-frequency analysis in electrical engineering area [1].

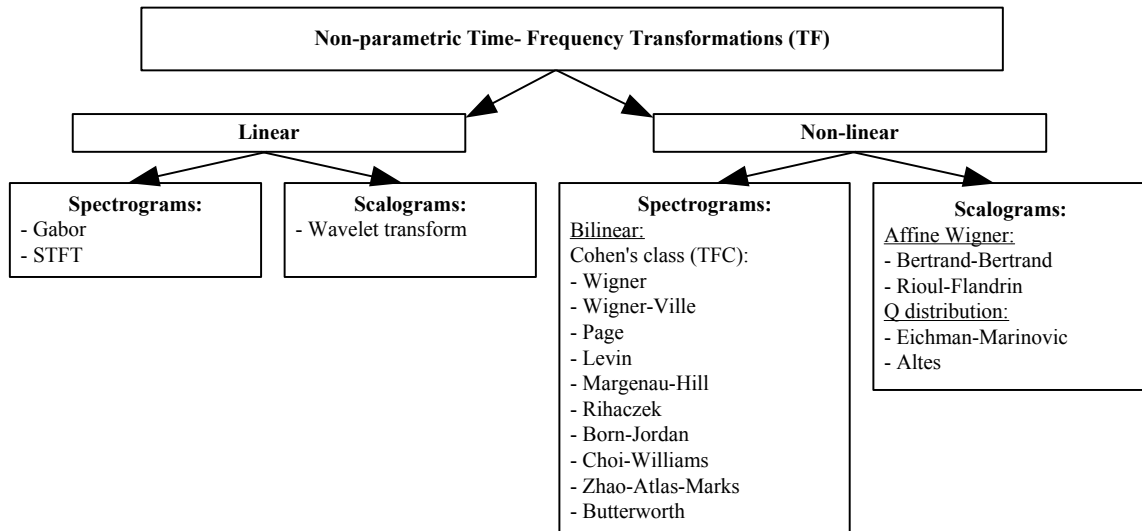


Figure 1 : Simplified division of non-parametric time-frequency transformations (TF).

The authors perceive a crucial need for better estimation of distorted electrical signal that can be achieved by applying the time-frequency analysis [6], [7]. Mentioned goal is strongly supported by an issue of energy quality and its wide-understood influence on energy consumers as well as producers. The proper estimation of the signal components is very important for control and protection tasks. The design of harmonics filters relies on the measurement of distortions in both current and voltage waveforms. For nonstationary area other techniques of signal processing methods can be considered such as wavelet transform or parametric methods with sliding window. Observing the effect of mentioned methods some limitations should be emphasised. Wavelet transform introduces variable level of frequency resolution which can be insufficient in case of wide range of observed time-varying spectrum. The parametric methods are characterised by high frequency resolution but for proper estimation some initial parameters are required. The crucial issue is the selection of model order which is related to number of estimated components. Proposed non-parametric bilinear transformations are characterised by fixed level of frequency resolution and do not require any initial parameters. The results of the methods can be also treated as a first suggestion for the selection of initial parameters for other signal processing methods.

In this paper some efforts was made to apply bilinear time-frequency transformations for analysis of non-stationary signals in electrical engineering. Firstly, chosen transformations were applied with comparison with short-time Fourier transform. The investigations were carried out using signal recorded in the supply system of dc arc furnaces. Then an idea of local frequency moments was introduced. To investigate the method several experiments were performed using simulated faults signals in transmission line. General purpose of the work is to emphasize the advantages and disadvantages

of proposed methods in point of their application for time-varying spectral estimation.

2 COHEN'S GENERALIZATION

Cohen defined a general class of bilinear transformation (TFC) introducing kernel function, $\phi_{\omega t}(\theta, \tau)$. The significance of Cohen's work is to reduce the problem of designing time-dependent spectrum to the selection of the kernel function [3],[4],[5],[8]:

$$TFC_x(t, \omega) = \int_{-\infty}^{+\infty} \int_{-\infty}^{+\infty} \int_{-\infty}^{+\infty} x\left(u + \frac{\tau}{2}\right) x^*\left(u - \frac{\tau}{2}\right) \cdot \phi_{\omega t}(\theta, \tau) e^{j\theta t} e^{-j\omega\tau} e^{-j\theta u} du d\tau d\theta \quad (3)$$

where: t – time, ω – angular frequency, τ – time lag, θ – angular frequency lag, u – additional integral time variable.

According to Cohen's generalization it is possible to obtain any bilinear time-frequency distribution by choosing suitable kernel function. Some examples of connections between distributions and their kernel functions were presented in Table 1. Performing the transformations brings two dimensional planes which represent the changes of frequency component, here called auto-terms (a-t). Unfortunately, bilinear nature of discussed transformations manifests itself in existing of undesirable components, called cross-terms (c-t). Cross-terms are located between the auto-terms and have an oscillating nature. It reduces auto-components resolution, obscures the true signal features and make interpretation of the distribution difficult. One crucial matter of kernel function is smoothing the cross-terms with preservation all useful properties of the distribution. The most prominent influence of cross-terms is then observed in case of Wigner distribution, where $\phi_{\omega t}(\theta, \tau) = 1$. Applying Gaussian kernel (CWD), "sinc" kernel (BJD) or cone-shaped kernel (ZAMD) brings smoothing effect on the equation level. It is possible to

Representation	Kernel function $\phi_{\omega t}(\theta, \tau)$	Equation of TFC _x (t, ω)
Wigner (WD)	1	$WD_x(t, \omega) \int_{-\infty}^{\infty} x\left(t + \frac{\tau}{2}\right) x^*\left(t - \frac{\tau}{2}\right) e^{-j\omega\tau} d\tau$
Wigner-Ville (WVD)	1	$WVD_x(t, \omega) \int_{-\infty}^{\infty} x_a\left(t + \frac{\tau}{2}\right) x_a^*\left(t - \frac{\tau}{2}\right) e^{-j\omega\tau} d\tau$, where $x_a(t)$ is analytic signal, obtained as a Hilbert transform of signal $x(t)$
Choi - Williams (CWD)	$e^{-\frac{(\theta\tau)^2}{\sigma}}$	$CWD_x(t, \omega) = \int_{-\infty}^{+\infty} \int_{-\infty}^{+\infty} \sqrt{\frac{\sigma}{4\pi \tau }} e^{-\frac{\sigma}{4}\left(\frac{t-u}{\tau}\right)^2} x\left(u + \frac{\tau}{2}\right) x^*\left(u - \frac{\tau}{2}\right) e^{-j\omega\tau} dud\tau$
Born-Jordan (BJD)	$\frac{\sin\left(\frac{\theta}{2}\tau\right)}{\frac{\theta}{2}\tau}$	$BJD_x(t, \omega) = \int_{-\infty}^{+\infty} \frac{1}{ \tau } \int_{t-\frac{ \tau }{2}}^{t+\frac{ \tau }{2}} x\left(u + \frac{\tau}{2}\right) x^*\left(u - \frac{\tau}{2}\right) e^{-j\omega\tau} dud\tau$
Zhao-Atlas-Marks (ZAMD)	$h(\tau) \tau \frac{\sin\left(\frac{\theta}{2}\tau\right)}{\frac{\theta}{2}\tau}$	$ZAMD_x(t, \omega) = \int_{-\infty}^{+\infty} h(\tau) \int_{t-\frac{ \tau }{2}}^{t+\frac{ \tau }{2}} x\left(u + \frac{\tau}{2}\right) x^*\left(u - \frac{\tau}{2}\right) e^{-j\omega\tau} dud\tau$

Table 1 : Some transformations of Cohen's class and their kernel functions [3],[4],[5].

introduce some additional operation which also bear fruit with smoothing, Figure 2.

The first one bases on multiplication of the signal with additional smoothing function $h(\tau)$. Applying equation (3) on such product leads to so called pseudo-time-frequency representation (PTFC) [4],[5],[8]:

$$PTFC_x(t, \omega) = \int_{-\infty}^{+\infty} \int_{-\infty}^{+\infty} x\left(u + \frac{\tau}{2}\right) x^*\left(u - \frac{\tau}{2}\right) \cdot h\left(\frac{\tau}{2}\right) h^*\left(-\frac{\tau}{2}\right) \phi_{\omega t}(\theta, \tau) e^{j\theta t} e^{-j\omega\tau} e^{-j\theta u} dud\tau d\theta \quad (4)$$

where: $h(\tau)$ – smoothing function, multiplied with signal.

Influence of the function $h(\tau)$ is the smoothing effect on original representation TFC along the frequency axis.

The second smoothing operation concerns convolution the pseudo-representation with next additional smoothing function $g(t)$ in time domain. It allows to smooth the cross-terms along time axis and is called smoothed pseudo-time-frequency distribution (SPTFC) [4],[5],[8]:

$$SPTFC_x(t, \omega) = \int_{-\infty}^{+\infty} g(t-u) PTFC_x(u, \omega) du \quad (5)$$

where: $g(t)$ – smoothing function, convoluted with pseudo-time-frequency representation.

It must be emphasised that mentioned additional operation have an influence on frequency and time resolution, accordingly. However, discussed approaches are characterised by independent tradeoff between time and frequency resolution. This feature clearly distinguishes described method in comparison with short-time Fourier transform, where the classic connection between time-frequency resolution and width of the smoothing window is inseparable [5].

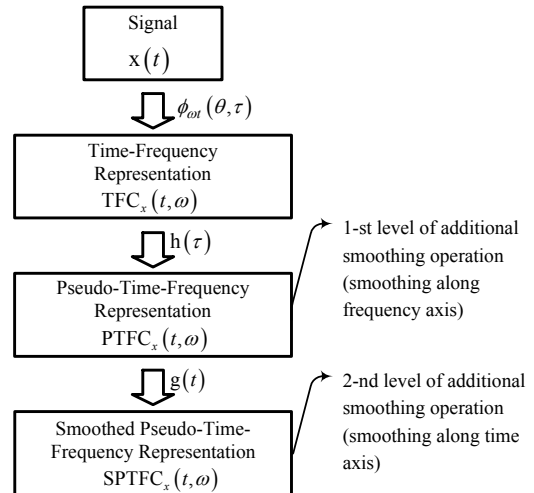


Figure 2 : Diagram of smoothing level operations

3 INVESTIGATION AREA

3.1 DC Arc Furnace

A typical dc arc furnace plant is shown in Figure 3. It consists of dc arc furnace connected to a medium voltage ac busbar with two parallel thyristor rectifiers that are fed by transformer secondary winding with Δ and Y connection, respectively.

The medium voltage busbar is connected to the high voltage busbar with a HV/MV transformer whose windings are $Y-\Delta$ connected. The power of the furnace is 80 MW. The other parameters are: Transformer T_1 - 80 MVA, 220kV/21kV; Transformer T_2 - 87 MVA, 21kV/0.638kV/0.638kV. Some filters are provided in the plants.

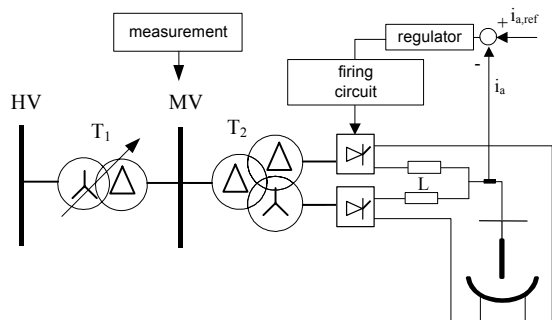


Figure 3 : Typical dc arc furnace plant.

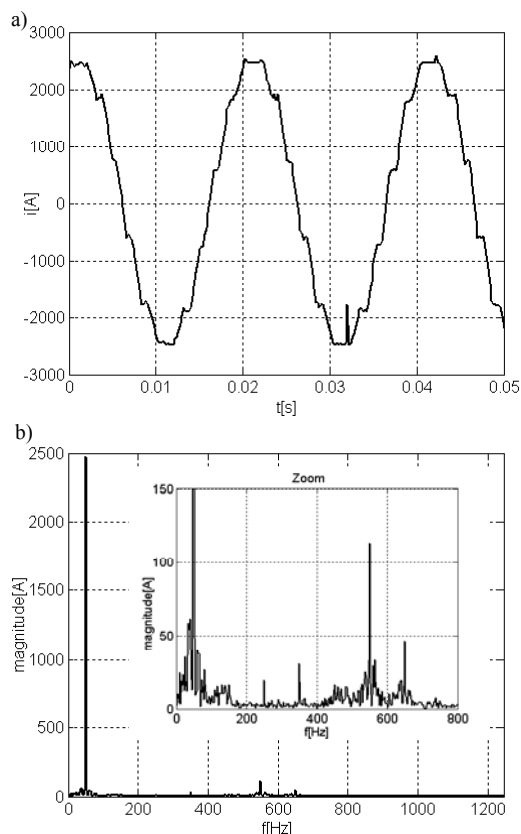


Figure 4 : Fragment of current waveform at MV busbar of the dc arc furnace (a) and its spectrum (b).

In the dc arc furnace, the presence of the ac/dc static converter and the random motion of the electric arc, whose non linear and time-varying nature is known, are responsible for significant perturbations, in particular waveform distortions and voltage fluctuations. In particular, the behaviour of the DC arc furnace can lead to the aperiodicity of AC electrical quantities, namely voltage and current at MV busbar. The phenomena correlated to the arc behavior are very complex. In [2] it has been shown that the DC arc voltage waveform has the aperiodic and irregular behaviour that characterizes every chaotic phenomenon. As an example, Figure 4 shows current waveform at MV busbar and its spectrum.

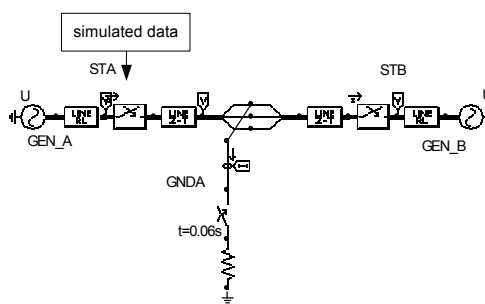


Figure 5 : Transmission line model

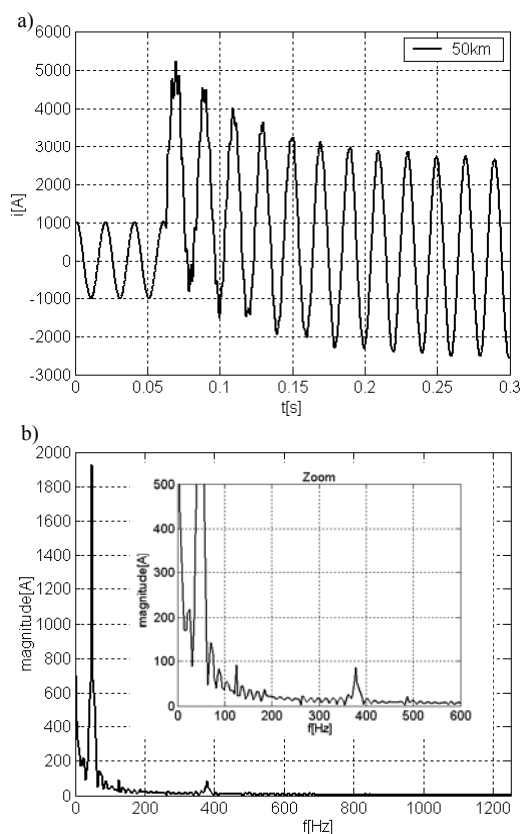


Figure 6 : Simulated current signal (a) and its spectrum (b) during ground fault in phase A, 50km from station STA.

3.2 Transmission line model

A model network has been simulated in EMTP-ATP packet, Figure 5. It includes two areas connected by a transmission line. The transmission line was modelled as a distributed parameters 400kV/185km line with positive sequence impedance of $Z_{L+}=(0.02762+j1.5745)\Omega/km$ and admittance of $B_{C+}=16.328\mu S/km$ as well as zero sequence impedance of $Z_{L0}=(0.275+j5.1295)\Omega/km$ and admittance of $B_{C0}=10.676\mu S/km$. The positive sequence Thevenine impedance of area "A" is $Z_{A+}=(1.3+j15.0)\Omega$ and zero sequence $Z_{A0}=(3.3+j18.0)\Omega$. The impedance of area "B" is $Z_{B+}=(2.2+j12.0)\Omega$ and $Z_{B0}=(2.5+j21.0)\Omega$ respectively.

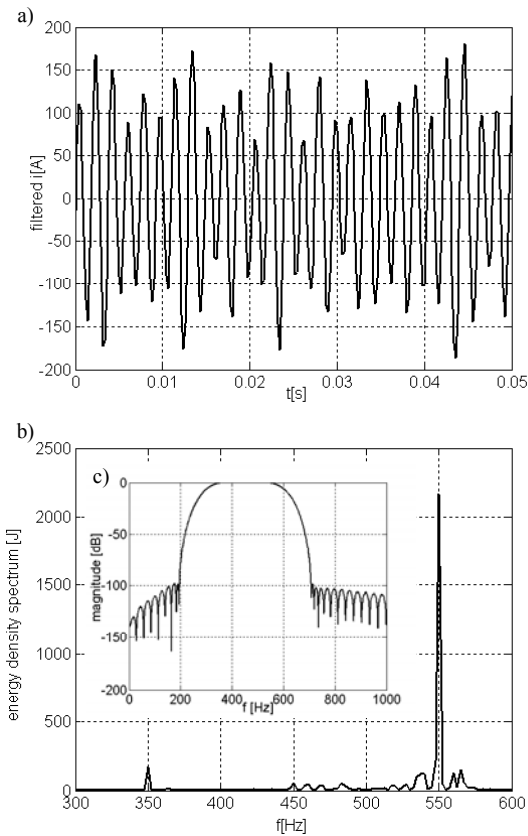


Figure 7: Fragment of current signal after band-pass filter 300-600Hz: (a) and its spectrum (b); (c) – magnitude characteristic of applied filter.

Described model allowed to simulate transient phenomena during the faults. Especially one-phase ground fault was chosen in point of the influence of the fault location. As an example, Figure 6 shows current waveform and its spectrum during ground fault in phase A, located 50km from station *STA* for occurring time $t=0.06s$.

4 INVESTIGATION RESULTS

4.1 DC Arc Furnace investigations

The measured current signal, which fragment is presented in Figure 4a, was taken into calculation. Sampling frequency amounted to 5kHz and recorded time range to 0.4s. First approach to the investigations provided calculation of signal's spectrum. Figure 4b shows the presence of the an ac/dc converter characteristic harmonics ($h=12p\pm 1, p=1,2,..$). Furthermore around the characteristic harmonics and around the fundamental component several interharmonics due to the arc fluctuations are visible. No details about the character of nonstationarity is visible.

Second approach considered applying joint time-frequency analysis in order to investigate non-stationary behaviour of frequency components. Due to wide range of spectrum we decided to demonstrate nonstationarity for only few selected items. Hence the band-pass filter (300-600Hz), Kaiser FIR, order 150, has been applied

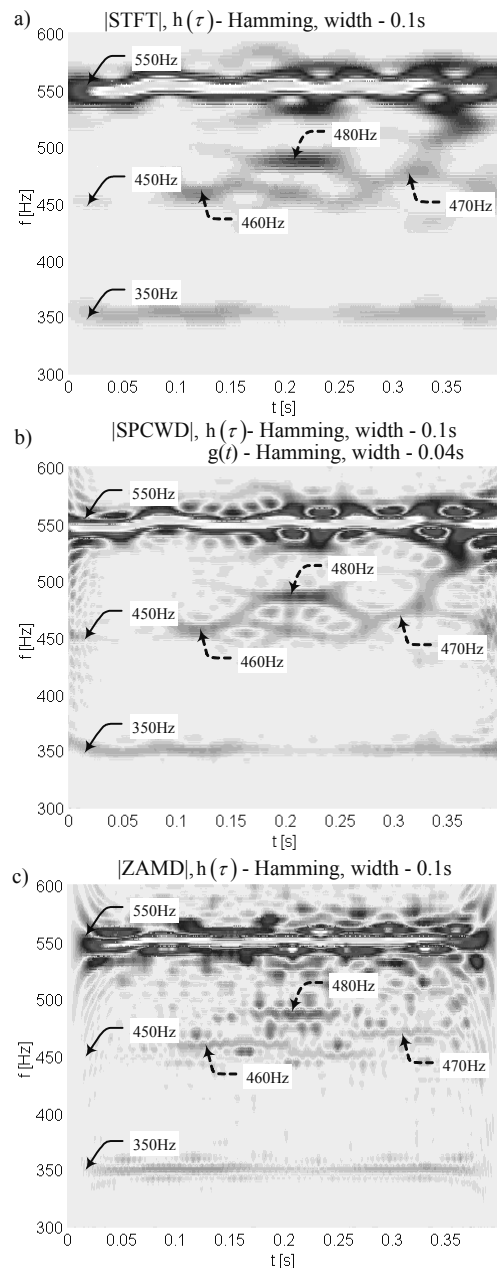


Figure 8: Frequency fluctuation represented on time-frequency plane when STFT (a), CWD (b) and ZAMD (c) was applied.

for initial limitation of the components, Figure 7. Then, time-varying spectrum was estimated using STFT with Hamming smoothing window that width equalled five periods of basic components (500 samples). For comparison some transformations belonging to Cohen's family was also applied. Smoothed pseudo-Choi-Williams Distribution (SPCWD) with factor $\sigma=0.05$ and Zhao-Atlas-Marks (ZAMD) were calculated using Hamming $h(\tau)$ and $g(t)$ function with window width amounted to five and two periods of basic component, respectively. Figure 8 contains time-frequency planes which allow to track the instantaneous character of frequency components. Some fluctuation of characteristic harmonics 350, 450, 550Hz was discovered.

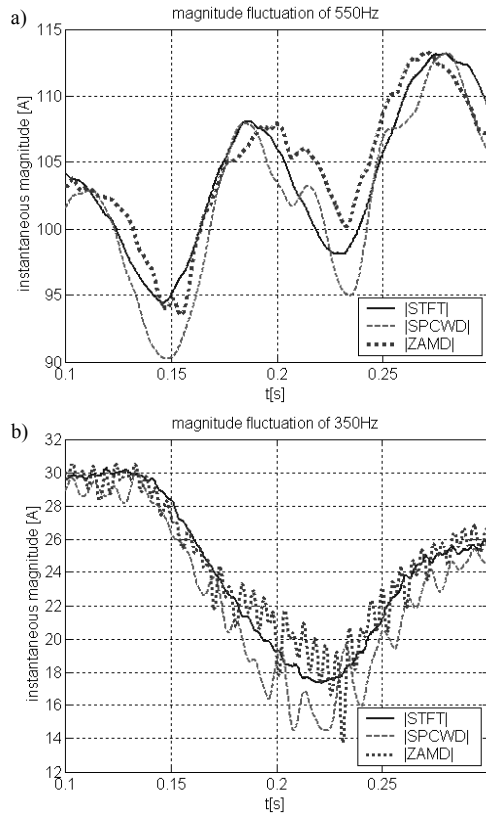


Figure 9 : Magnitude fluctuation of 550Hz (a) and 350Hz component (b) obtained using time-frequency representations from Figure 8.

Moreover, presence of interharmonics which appear around characteristic harmonics, especially around 450Hz, were also observed. Concentrating on the details we can recognize 460, 470, 480Hz. These components appear instantaneously according to the chaotic nature of dc arc furnace. Their magnitudes temporary even outstrip the characteristic harmonics. Comparing STFT with Cohen's family we can affirm improvement of time-frequency resolution.

One of the crucial advantages of time-frequency representations is providing information about the frequency and magnitude changes simultaneously. Thus, investigations of instantaneous magnitude of chosen components were possible. As an example, Figure 9 shows fluctuation of the magnitude of 550Hz and 350Hz components obtained using investigated methods. Presented results underline chaotic nature of dc arc furnaces phenomena.

4.2 Faults in transmission line model

Presented in this subsection results provide an idea to use one-dimensional characteristic of local frequency moment, calculated using two-dimensional time-frequency representation. The main idea of proposed approach introduces possibilities for further investigations of local frequency moment, treated as an index of nonstationarity. It brings novel directions for calculation of the beginning and duration time of transient states.

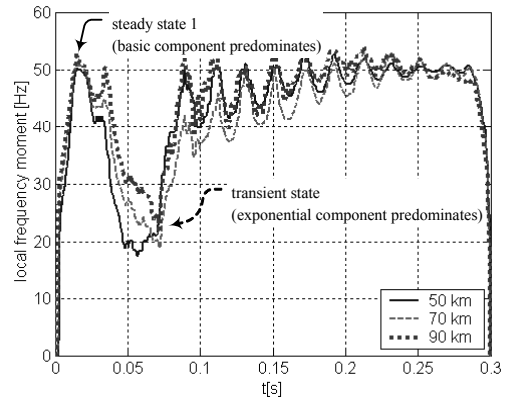


Figure 10 : Normalized local frequency moments of current signals during faults with different location obtained using WVD.

As an example, normalized local frequency moments of Wigner-Ville's distribution were calculated [10]:

$$\overline{\Omega_{WVD_x}^1}(t) = \frac{\int_{-\infty}^{+\infty} \omega WVD_x(t, \omega) d\omega}{\int_{-\infty}^{+\infty} WVD_x(t, \omega) d\omega} \quad (6)$$

Above equation can be then interpreted as a function which describes position of central point of the instantaneous spectrum for fixed time. It is worth emphasizing that following this interpretation, information about the frequency structure is lost. However information about the transient events is still preserved. The crucial significance of characteristic $\overline{\Omega_{WVD_x}^1}(t)$ is then the opportunity to apply it for detection of nonstationarity or duration time of transient states. Describing the local frequency moment we have to notice that cross-terms also take a part in the calculations. This influence manifest itself in oscillations around the true value of central point of spectrum which is achieved only when cross-term has zero-value. To avoid mentioned influence the authors propose to use median filter to suppress the oscillations. When small order of the filter is used no influence on dynamic of curve is achieved.

Simulated here one-phase ground faults manifest itself in existing the transient dc exponential component. Before the fault appears, instantaneous spectrum is concentrated in 50Hz. During the fault, from $t=0.06s$, we can recognize shifting the position of central point of the instantaneous spectrum from basic component to predominated exponential component, and then forwards basic components as a results of decaying transient state, Figure 10. The duration time of the transient state can be also clearly characterized.

5 CONCLUSIONS

It has been shown that the time-frequency representations of Cohen's class can be useful for parameter estimation of distorted, non-stationary signals. Significance effect of applied methods is possibilities to track instan-

taneous frequency and magnitude simultaneously. The dc arc furnace case confirms significance of the methods where fluctuation of frequency and magnitude as well as some interharmonics were detected.

One main deficiency of the methods are cross-term components which obscure real time-frequency representation. According to Cohen's generalization we can suppress the undesirable cross-terms by choosing the kernel function. If necessary, further smoothing operation can be applied using additional smoothing function. Discussed methods, however more computationally complex, are characterized by better frequency concentration than Fourier algorithm. Furthermore, characteristic for STFT tradeoff between time-frequency resolution and width of the smoothing window is here separable.

Results of discussed methods can be also treated as a first suggestion for the selection of initial parameters for other signal processing methods. For example, parametric high resolution methods require initial number of estimated components. Applying non-parametric method would deliver such information.

In further investigation the local frequency moments were calculated, which gave one-dimensional characteristics. Interpretation of obtained curve indicates position of central point of the instantaneous spectrum for fixed time. Following this interpretation, information about the frequency structure is lost, however information about the transient phenomena is still preserved. It makes possible to apply the discussed approach to detection and classification.

REFERENCES

- [1] Boashash B., *Time-Frequency Signal Analysis. Methods and Applications*, Longman Cheshire, Melbourne or Wiley Halsted Press, New York 1992.
- [2] Bracale A., Carpinelli G., Lauria D., Leonowicz T., Lobos T., Rezmer J., *On Some Spectrum Estimation Methods for Analysis of Non-Stationary Signals in Power Systems. Part I: Theoretical Aspects, Part II – Numerical applications*, 11-th International Conference on Harmonics and Quality of Power, Lake Placid, New York 2004, Session: Harmonic Propagation, paper no. - "f" and "g".
- [3] Cohen L., *Time – Frequency Distribution – A Review*, Proceedings of the IEEE, 1989, vol. 77, no. 7, pp. 941-981.
- [4] Hahn S. L., *A Review of Methods for Time-Frequency Analysis with Extension for Signal Plane-Frequency Plane Analysis*, Kleinheubacher Berichte, 2001, Band 44, pp. 163-182.
- [5] Hlawatsch F., *Linear and Quadratic Time-Frequency Signal Representations*, IEEE Signal Processing Magazine, 1992, pp. 21-67.
- [6] Leonowicz Z., Lobos T., Rezmer J., *Advanced spectrum estimation methods for signal analysis in power electronics*, IEEE Trans. on Industrial Electronics, June 2003, vol. 50, no. 3, pp. 514-519.
- [7] Lobos T., Leonowicz Z., Rezmer J., *Harmonics and Interharmonics Estimation Using Advanced Signal Processing Methods*, 9th IEEE Int. Conf. on Harmonics and Quality of Power, Orlando (USA) 2000, vol. I, pp. 335-340.
- [8] Loughlin P. J., Pitton J. W., Atlas L. E., *Bilinear Time-Frequency Representations: New Insights and Properties*, IEEE Transactions on Signal Processing, 1993. vol. 41, no. 2, pp. 750-767.
- [9] Papandreou-Suppappola A., *Application in Time-Frequency Signal Processing*, CRC Press, Boca Raton, Florida 2003.
- [10] Quian S., Chen D., *Joint Time-Frequency Analysis. Methods and Applications*, Prentice Hall, Upper Saddle River, New Jersey 1996.